Journal of Engineering Physics and Thermophysics, Vol. 81, No. 2, 2008

INVESTIGATION OF THE DYNAMICS OF RADIATIVE MICROPINCH DISCHARGES

A. S. Smetannikov

UDC 533.9

The dynamics of plasma cylinder compression by current pulses with a rise time of ~100 nsec in the Z-pinch geometry has been considered. The numerical simulation has been performed in the approximation of one-dimensional magnetic radiation gas dynamics. In the calculations, real thermodynamic, transport, and optical properties of the plasma have been used. The radiation transfer is described in the multigroup approximation by the photon energy. The calculations have been performed for a pinch in xenon (radius ~0.5 cm, energy E_0 = 10–30 J, maximum current ~30 kA). A detailed pattern of the dynamics of pinches has been investigated and the energy-to-radiation conversion efficiency has been determined.

The development of lithographic systems for the production of integrated circuits of a new generation (with a spatial resolution of elements less than 50 nm) is an important direction in the present investigations. To this end, sources of radiation in the region of extreme ultraviolet (EUV, wavelengths 10–15 nm) are needed. One of the most suitable techniques for their creation is the obtaining of a high-temperature plasma effectively emitting in this range (the electron temperature of the plasma therewith should be 20–50 eV). Such plasma can be obtained under the action of the laser radiation on the target or in pulsed electric discharges. The second technique is more efficient, since the efficiency of power supply energy conversion to plasma energy in electric discharges is much higher than under the action of laser pulses.

Most electric-discharge structures are based on the *Z*-pinch: electric discharge with a current pulse of 20–100 kA (rise time of ~100 nsec) in a cylindrical volume of radius 0.2–0.5 cm creates a plasma sheath which is compressed to the symmetry axis at a velocity of ~100 km/sec. As it decelerates on the symmetry axis, a dense hot plasma bunch is formed, and this plasma bunch is a source of radiation in the EUV region of the spectrum. The results of these works make it clear that it is necessary to study the processes proceeding in the acceleration and compression of plasma sheaths. Of particular interest is the efficiency of conversion of energy from the power supply to radiant energy. Since this problem contains many interrelated nonlinear physical processes, only individual aspects in a simplified statement can be considered by means of analytical solutions. A sufficiently complete theoretical picture of the compression dynamics can only be obtained by using numerical simulation.

The development of an EUV radiation source based on electric-discharge micropinches has been the subject of a number of recently published papers. In particular, radiation sources in such devices as capillary discharge, plasma focus, pseudospark discharge, *Z*-pinch, and other devices [1–8] based on lithium, xenon, or tin are being investigated. Note that in using an electric circuit consisting of a capacitor, an inductance coil, and a resistor closed to a pinch, it is extremely difficult to obtain a current rise time less than 1 μsec. Therefore, practically all the above structures use forming lines that make it possible to sharpen the voltage pulse and thus reduce the current rise time to a value of the order of 100 nsec. These forming lines consist of a whole set of inductors, resistors, and capacitors, whose parameters are not reported in the publications or are given incompletely. For the simulation of a discharge, the most important part of the circuit is its last link consisting of a capacitor, an inductor, and a resistor closed to the discharge gap. Therefore, in the calculation, the energy source is given by a usual *RLC*-circuit, whose parameters (capacitance *C*, inductance *L*, and resistance *R*) are selected so that the time dependence of current is reproduced with a fair accuracy, at least up to its first maximum.

A. V. Luikov Heat and Mass Transfer Institute, National Academy of Sciences of Belarus, 15 P. Brovka Str., Minsk, 220072, Belarus. Translated from Inzhenerno-Fizicheskii Zhurnal, Vol. 81, No. 2, pp. 216–222, March–April, 2008. Original article submitted May 31, 2007.

The plasma flow in some of these devices is non-one-dimensional (e.g., in the plasma focus in the pinch phase compression of the conical sheath occurs). At the same time, in most designs the discharge preserves the axial symmetry in compression and its parameters undergo a slight change in length, which makes it possible to describe the flow in the one-dimensional approximation. To simulate the discharge dynamics, one uses the system of equations of one-dimensional magnitude radiation gas dynamics [9]

$$\begin{gathered}\frac{\partial}{\partial t}\left(\frac{1}{\rho}\right)=\frac{\partial (rv)}{\partial m},\quad \frac{\partial r}{\partial t}=v,\quad \frac{\partial v}{\partial t}=-r\frac{\partial P}{\partial m}+f,\quad f=-\frac{jH}{\rho},\\ \frac{\partial \varepsilon}{\partial t}=-P\frac{\partial (rv)}{\partial m}+q-\frac{\partial (rS)}{\partial m},\quad q=\frac{jE}{\rho},\quad dm=\rho r dr,\\ \frac{\partial}{\partial t}\left(\frac{H}{\rho r}\right)=\frac{\partial E}{\partial m},\quad j=\sigma E=\frac{\rho}{4\pi}\frac{\partial (rH)}{\partial m}.\end{gathered} \tag{1}$$

The electron heat conductivity is neglected, since the energy transfer by the radiation turns out to be more significant. The power source is modeled by an *RLC*-chain closed to the plasma sheath, and the boundary conditions for the Maxwell equations from system (1) are defined by the electric circuit equations [9]

$$\begin{gathered}L\frac{dI}{dt}+RI-U+lE_N+\frac{\mu_0 l}{2\pi}\frac{d}{dt}\left(I\ln\frac{R_*}{R_N(t)}\right)=0,\\ \frac{dU}{dt}=-\frac{I}{C},\quad H(R_N,t)=\frac{2I}{R_N(t)},\end{gathered} \tag{2}$$

where $R_N(t)$ is the boundary of the region that carries the current; E_N and $H(R_N)$ are the electric and magnetic field strengths at this boundary; R_* is the radius of the reverse current flow; l is the charge length; I is the circuit current; $\mu_0 = 4\pi$ nH/cm. The initial conditions are: $U(0) = U_0$, $I(0) = 0$. The system of gas dynamics equations is closed by the equations of substance state in the form

$$P=nkT(1+x),\quad \varepsilon=\frac{3}{2}\frac{kT(1+x)}{M}+\varepsilon_i. \tag{3}$$

Here the ionization energy ε_i and the degree of ionization x are defined by the expressions

$$\varepsilon_i=\frac{k}{M}\sum n_i Q_i,\quad Q_i=\sum_{n=1}^{i} I_n,\quad x=\frac{\sum i\cdot n_i}{n}=\frac{n_e}{n},\quad n=\sum n_i.$$

The electrical conductivity is found as follows:

$$\begin{gathered}\frac{1}{\sigma}=\frac{1}{\sigma_1}+\frac{1}{\sigma_2},\quad \sigma_1=\frac{4\sqrt{2}}{\pi\sqrt{\pi}}\frac{(kT)^{3/2}\beta}{\sqrt{m_e}\,e^2 Z\Lambda},\quad \Lambda=\ln\left[1+\Lambda_1^2\right]^{1/2},\\ \sigma_2=\frac{3}{2}\sqrt{\frac{2}{\pi}}\frac{n_e e^2}{\sqrt{m_e kT}\sum n_0 s},\quad Z=\frac{\sum i^2 n_i}{\sum i n_i},\quad \Lambda_1=\frac{3}{2Ze^3}\left[\frac{(kT)^3}{\pi n_e}\right]^{1/2},\end{gathered} \tag{4}$$

where β is the correction coefficient for the electron-electron scattering. Here σ_1 corresponds to the Spitzer expression for a high-temperature plasma, and for a low-temperature plasma the Kauling expression (σ_2) is used when the scattering of electrons by neutral ions is dominant.

To find the radiation flux S, one has to solve the radiation transfer equation. Averaging it over the angles in the "forward–backward" approximation and over the frequency in the multigroup approximation, we obtain the system of equations [10]

$$\frac{1}{r}\frac{d}{dr}\left(rI_k^+\right)-\frac{I_k^+ + I_k^-}{2r}=2\left(\kappa_k' I_k^{\mathrm{eq}}-\kappa_k I_k^+\right),$$
$$\frac{1}{r}\frac{d}{dr}\left(rI_k^-\right)-\frac{I_k^+ + I_k^-}{2r}=-2\left(\kappa_k' I_k^{\mathrm{eq}}-\kappa_k I_k^-\right), \qquad (5)$$

where I_k^+ and I_k^- are the radiation intensities in the solid angle hemisphere directed in the positive and negative directions of the r-axis; k is the spectral group number; I_k^{eq} is the equilibrium radiation intensity in this spectral group; κ_k is the group absorption coefficient; $\kappa_k' I_k^{\mathrm{eq}}$ is the group emission coefficient. In this approximation the radiation flux is equal to

$$S=\sum S_k\,,\quad S_k=\pi\left(I_k^+ - I_k^-\right). \qquad (6)$$

The ionization composition of the plasma and the level populations have been calculated on the basis of the radiative-collisional model. From its viewpoint, the composition is defined by the equations

$$\frac{n_{i+1}}{n_i}=\frac{\beta_i}{\alpha_{i+1}^{\mathrm{r}}+n_{\mathrm{e}}\alpha_{i+1}^{3}+\alpha_{i+1}^{\mathrm{d}}}\,,\quad n_{\mathrm{e}}=\sum_i i n_i\,,$$

where β_i is the coefficient of ionization by ion-charge collision i; $\alpha_{i+1}^{\mathrm{r}}$, α_{i+1}^{3}, $\alpha_{i+1}^{\mathrm{d}}$ are the coefficients of radiative, three-particle, and dielectronic recombination for the $(i+1)$th ion, which were determined according to (11). The method of quantum-mechanical calculations of energy levels, ionization potentials, transition probabilities, etc., as well as of absorption and emission coefficients is described in [12]. For the numerical solution the system of equations (1)–(3) is completely approximated by the conservative difference scheme [9]. To solve the electrodynamics equations from (1) jointly with the circuit equations (2), the flow-fitting method is used [9]. With the help of this method the radiation transfer equations (5) are also solved. In calculating the radiation transfer, 40 spectral groups for the photon energy in the range of 0.01–14,000 eV are used.

The calculations have been performed for typical conditions of discharges, which are investigated as an EUV radiation source. The working medium is xenon with a pressure of 5–10 Pa, the initial radius of the plasma sheath $r_0 < 1$ cm, the level l is ~1 cm, the power supply voltage U_0 = 10–15 kV, the initial energy content E_0 = 5–50 J, the current maximum of 20–50 kA is attained in a time of about 100 nsec. Let us consider the results of the calculation for the following variants of plasma sheath acceleration and compression in xenon:

1) r_0 = 0.75 cm, l = 1.5 cm, the initial density $\rho_0 = 3\cdot10^{-7}$ g/cm^3; the circuit parameters are: L_{s} = 15 nH, C = 1.4 μF, R = 0.075 Ω, U_0 = 7 kV, R_* = 3 cm;

2) L_{s} = 9.6 nH, R = 0.045 Ω, l = 0.75 cm, the other parameters are same as in variant 1;

3) r_0 = 0.15 cm, l = 0.5 cm, $\rho_0 = 5\cdot10^{-6}$ g/cm^3; L_{s} = 20 nH, C = 50 nF, R = 0.08 Ω, U_0 = 25 kV, R_* = 0.5 cm.

Here the parameters of the first variant correspond to the device described in [5] and those of the third variant correspond to the device described in [8]. In the experiment, the current flow over the plasma sheath in the initial time interval is due to the gas breakdown. However, the energy input at the breakdown stage is small and the breakdown actually has a weak effect on the further development of the phenomenon if the azimuthal symmetry is observed (which is usually possible in experiment). Therefore, we will not calculate the breakdown kinetics but will simulate it giving some minimal electrical conduction of the gas (~$10^{-2}\ \Omega^{-1}\cdot$cm^{-1}). The skin-layer thickness ($\delta = c\sqrt{2\pi\omega\sigma}$) at such conductivity turns out to be large. Therefore, when a discharge of the capacitor bank is initiated, the electric field is homogeneous throughout the plasma sheath and the gas is heated practically uniformly. With increasing current the

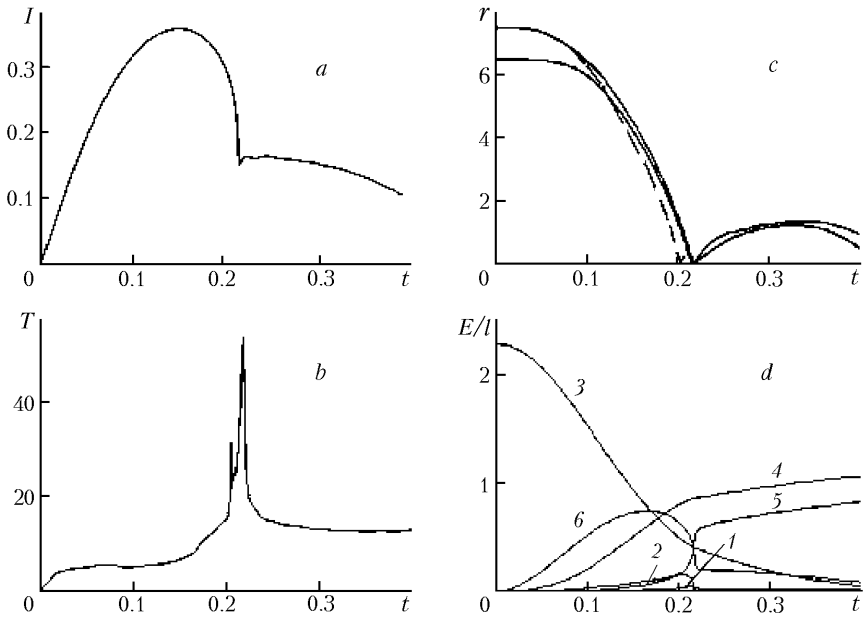

Fig. 1. Time dependence of the current (a), maximum temperature (b), plasma sheath and UV front boundaries (c), and energy per unit length (d) [1) internal, 2) kinetic, 3) capacitor, 4) resistor; 5) radiation, 6) magnetic] in the first variant of calculation. I, 100 kA; r, mm; T, eV; E/l, J/mm; t, μsec.

gas in the discharge is heated, its conduction grows, and the skin-layer thickness δ decreases. Therefore, the electric field is no longer homogeneous — its value is maximum near the outer boundary of the discharge where the most intensive heating occurs and a plasma sheath is formed.

Consider the results of the calculation of the first variant. The flowing current quickly heats the sheath (in ~15 nsec), the maximum temperature on the discharge layer increases to 5 eV. The current gradually grows, due to which the magnetic pressure increases and the sheath accelerates towards the symmetry axis. Before the compressing sheath there appears a shock wave (ShW) moving to the symmetry axis and somewhat leading it. The result of the calculation of the first variant are presented in Fig. 1. Solid lines in the r–t diagram show the motion of not only the outer boundary of the plasma cylinder, but also the particles located somewhat closer to the symmetry axis (for a better illustration of the compression dynamics), and dashed lines show the shock wave. At the stage of convergence to the axis the energy gradually goes from the capacitor to the inductor and the kinetic energy of the sheath, and an appreciable part of it is lost on external resistor. Note that the maximum temperature of the plasma at this stage changes slightly and remains at the level of 5 eV. The current reaches a maximum of 37 kA in 160 nsec and then begins to decrease. In 170 nsec the sheath radius markedly decreases and the gas compression leads to an increase in the maximum temperature to 17 eV (200 nsec). At this instant of time the ShW arrives at the symmetry axis, which causes a sharp temperature rise to 34 eV, and reflects from it. The plasma sheath continues to compress and in 215 nsec the greatest compression on the axis occurs. The maximum temperature on the discharge layer rapidly increases and reaches a value of 55 eV. The sheath decelerates, reflects from the axis, and then begins to recede from it. The radiation loss of energy in the process of sheath cumulation on the axis rapidly grows and reaches 0.7 J/mm (230 nsec). The discharge emits about 30% of the energy, and a considerable portion thereby is due to the hard ultraviolet radiation. Practically the whole of the kinetic energy of the sheath and part of the energy previously stored in the inductor are converted to radiant energy. About one half of the initial energy is expended in heating the external resistor. The outer boundary of the plasma sheath gradually recedes from the axis and then its expansion is decelerated by the magnetic forces, since the current is still high (15 kA). By the instant of time 320 nsec it is at a distance of 1.5 mm and begins to accelerate again towards the symmetry axis. Subsequently secondary compression of the pinch occurs (430 nsec). Note the characteristic feature of the time dependence of current: near the moment of sheath cumulation on the axis the current drops sharply to a value equal to 1/3–2/3 of the maxi-

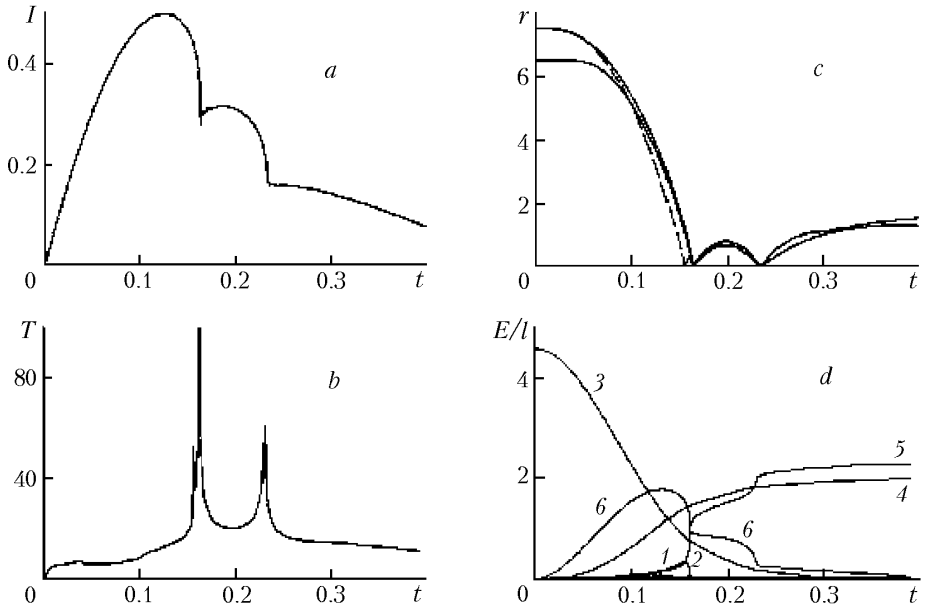

Fig. 2. Time dependence of the current (a), maximum temperature (b), plasma sheath and UV front boundaries (c), and energy per unit length (d) in the 2nd variant of calculation. Notation 1–6 same as in Fig. 1. I, 100 kA; r, mm; T, eV; E/l, J/mm; t, μsec.

mum. Such behavior of the current is observed in experiments ("stall" of current) [5, 7] and is due to the rapid change in the inductance and resistance of the plasma caused by compression. Write the first equation of (2) in a different form:

$$L_s \frac{dI}{dt} + I\frac{dL_s}{dt} + RI - U + lE_N = 0\,, \quad L_s = L + \frac{\mu_0 l}{2\pi}\ln\frac{R_*}{R_N(t)}\,.$$

It is seen that the quantity dL_s/dt acts as some resistance. In compression it rapidly increases and can become higher than the external resistance R since

$$\frac{dL_s}{dt} = \frac{d}{dt}\frac{\mu_0 l}{2\pi}\ln\frac{R_*}{R_N(t)} = \frac{\mu_0 l}{2\pi}\frac{v_N(t)}{R_N(t)}\,.$$

Moreover, at the final stage of pinch compression the plasma cylinder resistance rapidly increases, which can also influence the behavior of current [13]. In simulating pinches, the electric circuit equations are often not taken into account and the time dependence of current is given. However, it is possible to obtain such behavior of the current in the calculation only by solving the self-consistent problem when the current is found from the electric circuit equations in which the pinch acts as one of its elements having time-variable parameters in accordance with the compression dynamics.

The results of the calculation of the second variant of the discharge are presented in Fig. 2. Qualitatively, the discharge dynamics pattern is as before. The current reaches a maximum of 50 kA (115 nsec), which is a somewhat larger value than in the first variant. The plasma sheath compresses near the symmetry axis in 165 nsec, and the temperature increases to 100 eV. By this moment the current rapidly decreases to a value of 30 kA, after which the plasma sheath reflects from the axis, expands, and decelerates on a radius of 1 mm. Then its secondary compression on the axis (230 nsec) occurs, which leads to a current drop to 15 kA. In the second compression, the maximum temperature appears to be rather high, ~60 eV. Subsequently, the sheath reflects from the axis and expands outside, and the current slowly decreases. Note that the maximum temperature between the first and the second compression re-

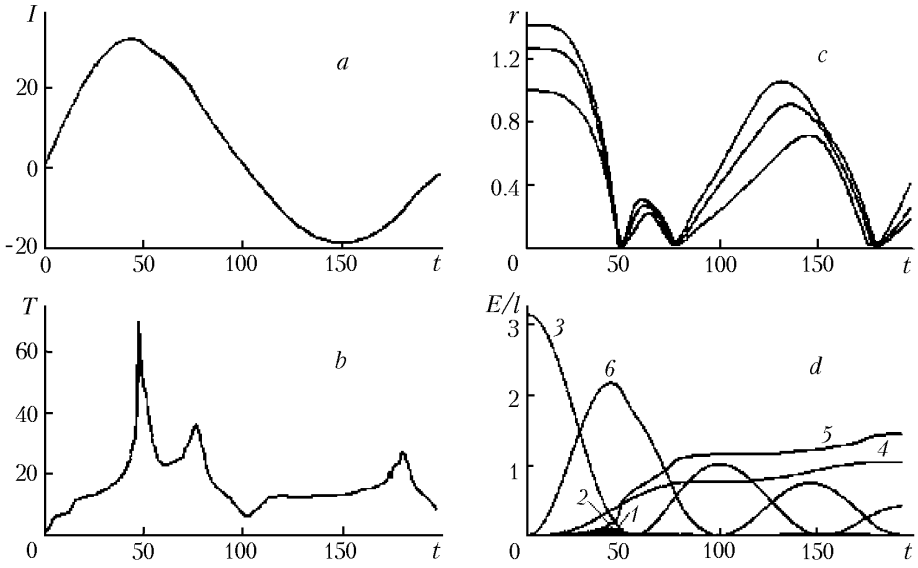

Fig. 3. Time dependence of the current (a), maximum temperature (b), plasma sheath and UV front boundaries (c), and energy per unit length (d) in the 3rd variant of calculation. Notation 1–6 same as in Fig. 1. *I*, 100 kA; *r*, mm; *T*, eV; *E*/*l*, J/mm; *t*, nsec.

mains rather high, over 20 eV. By the instant of time 400 nsec the energy emitted from the discharge accounts for about one half of the energy input into the discharge and slightly exceeds the external resistance losses. Note that in the time interval between the first and the second compression of the pinch the radiant energy almost doubles. Comparing to the first variant, note that a decrease in the inductance and external resistance of the circuit leads to an increase in the energy input into the plasma and in the efficiency of its conversion into radiant energy.

Consider the results of the calculation of the third variant (Fig. 3). The qualitative pattern of the discharge dynamics is similar to the previous variants; however, there are certain differences. The current grows faster and reaches its maximum in 50 nsec (32 kA). Joule energy release leads to a heating of the gas and in 15 nsec the maximum temperature does not exceed 10 eV. An increase in the magnetic pressure causes an acceleration in the heated gas sheath towards the symmetry axis. Since the initial radius of the sheath is much smaller than in the previous variants of the calculation, its compression occurs faster, in 48 nsec. At the compression stage of the pinch a large portion of energy from the capacitor is transferred to inductance energy, a certain portion (~15%) is expended in heating the external resistor, and a still smaller portion changes to kinetic energy and is emitted from the discharge. In this variant, pinch compression causes no drop of current, which is due to the higher initial density and the smaller initial radius. In compression, the temperature grows rapidly and reaches a maximum of 70 eV (48 nsec). After that the pinch expands and decelerates on r = 0.3 mm and the maximum temperature decreases to 22 eV. Since the current is not yet high (~20 kA), the pinch compresses for the second time (in 75 nsec) and the temperature increases again (to 35 eV). It should be noted that in the time interval between the first and the second compression the energy emitted from the discharge almost doubles. Then reflection from the axis occurs and the pinch expands for a long time, since the current passes through zero and the magnetic pressure is low. Subsequently, the current passes through the minimum in 150 nsec and the increase in the magnetic pressure causes deceleration and termination of expansion. Then the pinch compresses once again (180 nsec) and the temperature increases to 25 eV. The discharge characteristics obtained in the calculation (time dependence of current and voltage, moments of three compressions of the pinch, etc.) are in fair agreement with the experimental data of [8]. By the instant of time 200 nsec the energy emitted from the discharge amounts to 45% of the initial energy, and much less energy is expended in heating the external resistor. In this variant of calculation, the efficiency of energy transfer into the plasma and its conversion to radiation are fairly high.

In investigating the given discharges, the composition of the radiation obtained is important. Figure 4 shows the change with time in the radiant fluxes from the discharge in 13–19 spectral groups (boundaries 54.2–66–88.6–93.5–95.4–107.4–182.2–237 eV) for the second and the third variants of calculation. This figure shows that at pinch

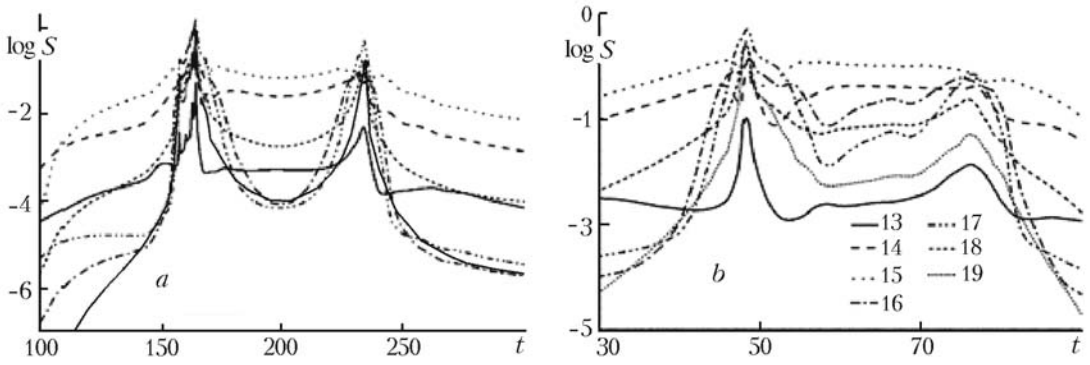

Fig. 4. Radiation fluxes in 13–19 groups for the 2nd (a) and 3rd (b) variants of calculation. S, 100 MW/cm^2; t, nsec.

compression moments maximum radiant fluxes are attained in 15–17 spectral groups. And their value therewith exceeds 100 MW/cm^2 in the first compression and somewhat less in the second one.

The results of the calculations performed show that the considered discharges are intensive sources of radiation in the ultraviolet region of the spectrum, and the maximum radiant fluxes can reach 100 MW/cm^2. A correct description of the discharge dynamics requires a self-consistent solution of the problem with the determination of the current from the electric circuit equations. An important feature of the considered discharges is the double compression of the pinch with a short interval between compressions (so that the maximum temperature does not drop below 20 eV). This makes it possible to markedly increase the radiant energy and transfer to the radiation more than 40% of energy by matching the parameters of the plasma sheath and the current pulse.

NOTATION

c, velocity of light; $E \equiv E_z$ and $H \equiv H_\varphi$, components of the electric (axial) and magnetic (azimuthal) field strengths; e, electron charge; f, force acting on the plasma due to the current-magnetic field interaction; I_n, ionization potentials; j, current density; k, Boltzmann constant; m, Lagrangian (mass) coordinate; M, atomic mass; n_e, n_0, n_i, concentrations of electrons, atoms, and ions of the ith degree of ionization; n, concentration; P, pressure; q, Joule energy release; r, radius; R, L, and C, resistance, inductance, and capacitance of the circuit; S, radiant flux; s, transport cross-section of the electron scattering by atoms; t, time; T, temperature; U, capacitor bank voltage; v, velocity; Z, average charge; α^r_{i+1}, α^3_{i+1}, α^d_{i+1}, coefficients of radiative, three-particle, and dielectronic recombination; β_i, collisional ionization coefficient of the ion; ε, specific internal energy; Λ, Coulomb logarithm; ρ, density; σ, electrical conduction; ω, frequency. Subscripts: e, electron; 0, neutral; r, radiative; 3, three-particle; d, dielectronic; z, axial; φ, azimuthal; s, total; eq, equilibrium; N, point number.

REFERENCES

1. W. N. Partlo, I. V. Fomenkov, R. Oliver, et al., Development of an EUV (13.5 nm) light source employing a dense plasma focus in lithium vapor, *Proc. SPIE*, **3997**, 136–156 (2000).
2. R. M. Ness and W. N. Partlo, Solid-state pulsed power module design for a dense plasma focus device for semiconductor lithography applications, in: *Proc. 13th IEEE Pulsed Power Plasma Conf.*, Las Vegas, Nevada (2000).
3. K. Bergmann, O. Rosier, R. Lebert, et al., A multi-kilohertz pinch plasma radiation source for extreme ultraviolet lithography, *Microelectronic Eng.*, **57–58**, 71–77 (2001).
4. G. Schriever, U. Stamm, K. Gabel, et al., High-power EUV sources based on gas discharge plasmas and laser produced plasmas, *Microelectronic Eng.*, **61–62**, 83–88 (2002).
5. V. M. Borisov, A. Yu. Vinokhodov, A. S. Ivanov, et al., A high-power gas discharge source of VUV (13.5 nm) radiation, *Fiz. Plazmy*, **28**, No. 10, 952–956 (2002).

6. L. Juschkin, A. Chuvatin, S. V. Zakharov, et al., EUV emission from Kr and Xe capillary discharge plasmas, *J. Phys. D: Appl. Phys.*, **35**, No. 3, 219–227 (2002).
7. E. R. Kieft, A. M. van der Mullen, G. M. W. Kroesen, et al., Characterization of a vacuum-arc discharge in tin vapor using time-resolved plasma imaging and extreme ultraviolet spectrometry, *Phys. Rev. E*, **71**, No. 2, 026409-1-026409-7 (2005).
8. S. Katsuki, A. Kimura, A. Hongo, et al., Z-pinch EUV source driven by 100 ns current pulses, *Second EUVL Symposium*, Antwerpen, Belgium (2003), 09/30-10/01, Poster-086.
9. A. A. Samarskii and Yu. P. Popov, *Difference Methods of Solving Gas Dynamics Problems* [in Russian], Nauka, Moscow (1980).
10. G. S. Romanov and A. S. Smetannikov, Numerical simulation of a layered pulsed discharge with allowance for the energy transfer by radiation, *Zh. Tekh. Fiz.*, **52**, No. 9, 1756–1762 (1982).
11. L. A. Vainshtein, I. I. Sobel'man, and E. A. Yukov, *Excitation of Atoms and Broadening of Spectral Lines* [in Russian], Nauka, Moscow (1979).
12. M. A. El'yashevich, F. N. Borovik, S. I. Kas'kova, et al., Thermodynamic functions and absorption coefficients of bismuth and xenon plasmas, *Proc. 4th All-Union Conf. "Emitting Gas Dynamics"* [in Russian], Vol. 1, MGU, Moscow (1981), pp. 129–139.
13. G. S. Romanov, A. S. Smetannikov, Yu. A. Stankevich, and V. I. Tolkach, Dynamics of the Z-pinch with a light liner. II. Single-envelope liners and the anomalies of the cumulation stage, *Inzh.-Fiz. Zh.*, **59**, No. 4, 635–641 (1990).